

## Computation of SAR in Cell Culture Flasks Exposed to 900 MHz GSM Type Signals in a Modified TEM Cell

Robert L McIntosh, Raymond J McKenzie, Steve Iskra, Amico Carratelli, and Paul Standaert  
Telstra Research Laboratories, Clayton, Victoria, 3168, Australia  
[robert.l.mcintosh@team.telstra.com](mailto:robert.l.mcintosh@team.telstra.com)

**Abstract:** In order to provide rigorous dosimetry for *in vitro* studies, Telstra Research Laboratories has developed a modified transverse electromagnetic cell exposure system. The system acts as a chamber for experiments in which a human cell culture exists as a very thin monolayer adhered to the bottom of a plastic culture flask under a layer of several millimetres of RPMI nutrient medium while incubated in a controlled atmosphere. A key to the rigour of any experiment seeking to investigate possible effects of electromagnetic energy on living systems is to ensure that the exposures used are accurately known, and to achieve this, numerical methods for the challenging task of characterising the SAR profile in the medium have been developed. This paper describes salient aspects of the development and analysis of the system.

**Keywords:** FDTD modelling; RF exposure; TEM cell; SAR; GSM

### 1. Introduction

To enable the future investigation of possible biological effects of mobile phone exposure, this paper considers an experimental setup where a human cell culture can be exposed to 900 MHz GSM type radiofrequency (RF) signals. The exposure system consists of a modified Crawford transverse electromagnetic (TEM) cell (Crawford 1974), which is supplied with a simulated GSM mobile phone type signal at 20 W peak power (900 MHz RF signal pulsed at 1/8 duty cycle for 2.5 W average power). The cell culture is placed in the TEM cell in standard *Falcon*<sup>TM</sup> 25 cm<sup>3</sup> plastic culture flasks and resides as a very thin monolayer (a few microns) at the bottom of 6 mm of the nutrient RPMI-1640 (Roswell Park Memorial Institute) while incubated in a 37 °C CO<sub>2</sub> atmosphere. This setup is similar to that discussed in French and Blood 2002 which investigated possible gene expression changes in live human astrocytes.

For this situation, the specific energy absorption rate (SAR) (W/kg) is commonly accepted to be the most appropriate metric for determining RF exposure. SAR can be determined at any point in a medium from the *E*-field (V/m) at that point:

$$SAR = \frac{\sigma |E|^2}{\rho} \quad (1)$$

where  $\sigma$  is the conductivity (S/m) and  $\rho$  is the mass density (kg/m<sup>3</sup>).

Many RF exposure systems rely on measurements of average absorption within the target material to determine the SAR. In a TEM cell, the actual SAR at any given point in the exposed medium will differ markedly from the average value. The geometry used here, where the height (*h*) of the medium coincides with the direction of the incident electric (*E*) field, ensures that there is the essential uniformity in SAR on the bottom layer of the RPMI medium where the cell culture resides. However, it also means that SAR typically varies quadratically with *h* within the medium (see Burkhardt et al. 1996, Guy et al. 1999, Samaras et al. 2000, and Schönborn et al. 2001). This makes it critical that accurate computational techniques are used to provide a good estimate of SAR (especially on the bottom layer).

### 2. Choice and Design of Exposure Chamber

To achieve well controlled and characterised RF exposures has been a concern in many previous studies. References Guy et al. 1999, Kuster and Schönborn 2000, and Schönborn et al. 2000 and 2001, discuss exposure requirements and the merits of various exposure systems. Such systems include waveguides, radial transmission lines (RTL), TEM cells, Gigahertz TEM (GTEM) cells, and free-field exposure in anechoic chambers.

Based on considerations of physical size, experimental needs, and required field characteristics, a TEM cell was chosen. A TEM cell provides uniform incident plane wave exposure conditions, useful for simplifying analysis, as long as each culture flask is placed in a central position and the absorbing medium is not too thick (see Crawford and Workman 1979, Burkhardt et al. 1996, Popovic et al. 1998, and Schönborn et al. 2001) (Figure 1). Modifications included provision of adequate ventilation in the 37 °C CO<sub>2</sub> incubator (Figure 2); access ports and inserts to allow placement of the two flasks at the midpoint of the top half of the TEM cell (Figure 3); and fixtures to allow

ingress and accurate location of fluoroptic temperature probes (Figure 4). The measured return loss of the input signal was greater than 30 dB. To ensure CO<sub>2</sub> diffusion and suitable power efficiency the height of the RPMI was chosen to be 6 mm. Total absorbed power with the TEM cell loaded with two flasks containing the RPMI was less than 4% of forward power, indicating that the TEM field conditions were maintained within the TEM cell.

### 3. Determination of SAR

The commercially available computational software XFDTD (Remcom 2003) was used to determine the SAR profile in the RPMI (Figure 5). The SAR was used to report the background energy level in which the cell culture was placed and also to validate the setup through the resultant temperature estimation. XFDTD uses the finite-difference method (see, for example, Kunz and

Luebbers 1993). A computational mesh of the 6 mm medium was constructed with cubical cells of length 0.5 mm. The conductivity of RPMI was set at 1.8 S/m, relative permittivity 73.2, and density 1000 kg/m<sup>3</sup>. The incident field frequency was 900 MHz with the *E*-field polarised in the vertical direction.

For the supplied plane wave signal (*E*-field 214 V/m peak amplitude, equivalent to 2.5 W average power in the TEM cell), the calculated peak SAR on the bottom of the medium was 0.20 W/kg. The average SAR on this level was found to be 0.18 W/kg. Figure 5 highlights the uniformity of SAR on the bottom layer, and the non-uniformity in the 6 mm vertical direction (this profile is consistent with published results Burkhardt et al. 1996, Guy et al. 1999, Pickard et al. 1999, Samaras et al. 2000, and Schönborn et al. 2001).

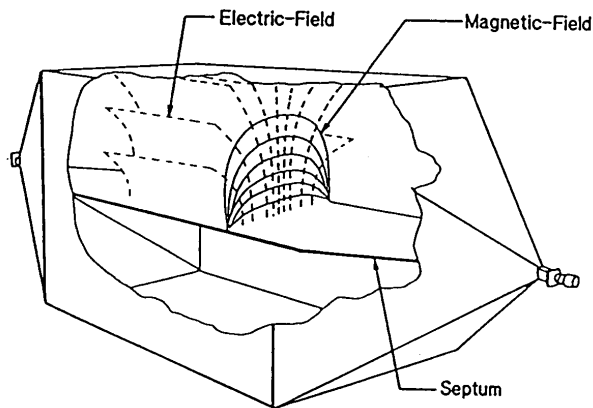


Figure 1. The electric and magnetic fields within a TEM cell, with a plane wave type structure at the midpoint of the top half.

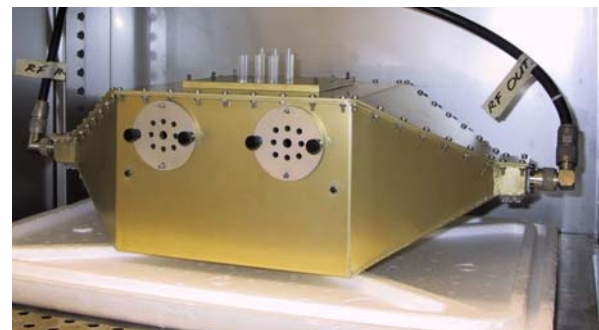


Figure 2. TEM Cell placed in the incubator (with ventilation holes shown).

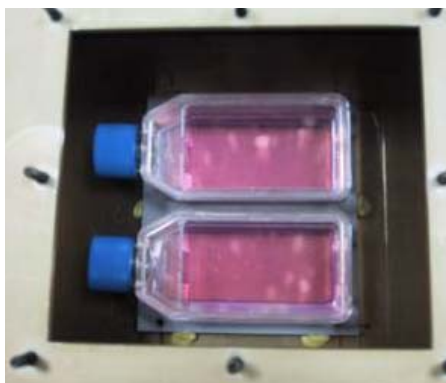


Figure 3. Two culture flasks, each filled with 6 mm of RPMI, placed in the middle of the top half of the TEM cell.

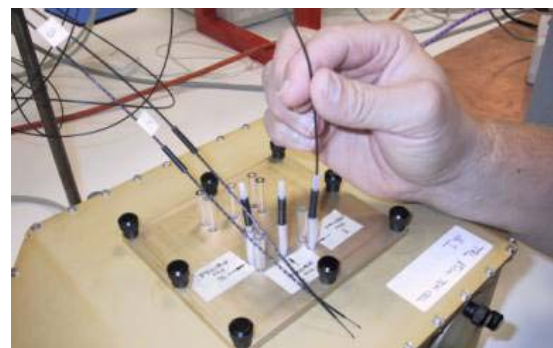


Figure 4. The placement of fluoroptic temperature probes. Three probes were placed at distinct regions of one flask. Each tip was situated in the medium, 0.5 mm above the flask bottom.



Figure 5. SAR profile in the RPMI medium. top: Slice through the middle (note the medium in the neck of the flask on the left). bottom: Bottom layer where cell culture resides.

An uncertainty analysis suggested the actual SAR values should agree with these values to within  $\pm 35\%$ . The main contributing factors to the possible error are the input power (accurate to within  $\pm 25\%$ ; has a linear influence on the calculated SAR), height of the medium (accurate to within  $\pm 0.5$  mm resulting in a possible  $\pm 17\%$  error; quadratic), and the conductivity ( $\pm 10\%$ ; approximately linear). The modelling has also highlighted the significant influence of the meniscus due to the  $E$ -field polarisation (see also Guy et al. 1999, Schönborn et al. 2001, and Schuderer and Kuster 2003). The addition of the meniscus, 1 mm high and 1 mm in from the edge, as shown in the top right of Figure 5, lead to a 5% increase in SAR on the bottom layer.

Note that SAR has only been determined in the nutrient medium. The method of determining SAR without including the cell culture layer itself is consistent with work by other investigators in this field (see, for example, Schönborn et al. 2000 and 2001). To also determine SAR in the actual cell culture is a difficult task since the height of this layer is just a few microns. If the cell culture (assumed to be human brain cells) is included in the model as an infinitely thin planar layer at the bottom of the medium (with conductivity 0.77 S/m and relative permittivity 45.8 as for average brain (Gabriel 1996)) then the peak SAR at the bottom is reduced to 0.14 W/kg. If instead, the cell culture is modelled by the bottom 0.5 mm layer of mesh cells, then the peak is 0.10 W/kg. The actual value is likely to lie somewhere in this range, so long as the dielectric values for the cell culture have been appropriately chosen in the models. Better consideration of this issue of the SAR at the cell culture layer may be possible as improved modelling techniques become available.

The efficacy of using a plane wave incident field to simplify the analysis was confirmed by an XFDTD

model of the rectangular central portion of the TEM cell (using a ‘TEM Excitation Plane’). The resultant electromagnetic fields have the required plane wave type structure at the position of the flasks.

#### 4. Comparison with, and Application of, the Burkhardt Formula

In Burkhardt et al. 1996, an analytical formulation is derived that provides SAR as a function of height (thickness),  $h$ , of the medium (which is taken to be in the direction of the incident field  $E$ ). It is assumed that the geometry can be simplified to that of a thin conductive sheet. This enables a “... separation between ‘capacitive’ and ‘inductive’ coupling ... the capacitively induced part of the  $E$ -field [ $E_{cap}$ ] is normal and the inductively induced part [ $E_{ind}$ ] is parallel to the surface of the [sheet].” The formula is

$$\begin{aligned} SAR(z') &= \frac{\sigma}{\rho} (|E_{ind}|^2 + |E_{cap}|^2) \\ &= \frac{\sigma}{\rho} |E|^2 \left( \left( \frac{\mu\omega z'}{Z_0} \right)^2 + \frac{1}{|\epsilon_k|^2} \right) \end{aligned} \quad (2)$$

where it is assumed that the centre of the bottom of the sheet (lying in the  $x$ - $y$  plane) is at the origin of a Cartesian coordinate system, and  $z' = z - h/2$ ,  $\omega = 2\pi f$ ,  $f$  is the frequency,  $\epsilon_k = \epsilon_r - i\sigma/(\epsilon_0\omega)$ , and  $Z_0 = 377 \Omega$ .

To consider the accuracy of the Burkhardt formula with  $h$ , XFDTD models of finite sheets were constructed at a series of values. In each XFDTD model, the sheet was of dimensions 100 mm  $\times$  100 mm and was 12 mesh cells high, and the material and field properties were

identical to those above. For each method, the SAR values at the bottom of the sheet (centrally placed in the XFDTD model) were compared. The comparison indicated that there was close agreement for a 4 mm high sheet (Burkhardt 0.0648 W/kg, XFDTD 0.0634 W/kg), around a 10% difference at 6 mm (0.138 W/kg, 0.152 W/kg), with the accuracy diminishing at 12 mm (0.535 W/kg, 1.30 W/kg). The analysis also highlighted that the desired uniformity over the bottom layer also diminishes significantly as  $h$  increases.

The formula thus provides a coarse validation method for checking the results from an XFDTD analysis of the SAR in a flask. In particular, at 6 mm, the Burkhardt formula gives the value of 0.138 W/kg (the sheet is the only possible analytic geometry) compared with the XFDTD value 0.20 W/kg (calculated above for the flask).

However, the formula offers a very prompt method to calculate approximate SAR values (an XFDTD calculation takes a few hours), which is useful in initial experimental design. It can also be used to test the sensitivity of input parameters. For example, the formula indicates that SAR varies quadratically with  $h$  (closely approximating the profile of the vertical slice in Figure 5). Since the cells reside on the bottom of the medium, this emphasises the need to choose and measure this parameter with great care.

### 5. SAR Validation through Temperature Measurement and Modelling

The efficacy of using XFDTD to determine the SAR profile was also confirmed through comparison of physical measurements of the resultant thermal rise in the medium with numerically calculated estimates based on the predicted SAR. Thermal RF dosimetry is based upon the equation

$$\rho c \frac{\partial T}{\partial t} = K \nabla^2 T + \rho SAR \quad (3)$$

where  $c$  is the specific heat capacity, and  $K$  is the thermal conductivity.

A standard approach in the determination of SAR is to ignore the conduction term  $K \nabla^2 T$  in equation 2 and measure the initial rate of temperature increase  $\partial T/\partial t$  (see, for example, Rowley and Anderson 1999). However, this approach is not possible in this case due to the high vertical SAR gradient, unless either highly sensitive temperature probes are used or the input power is significantly increased (see Moros and Pickard 1999, Pickard et al. 1999, and Samaras et al. 2000). (An alternative is to use equation 1 and use an  $E$ -field probe with a tip that is small enough and positioned so that it does not disrupt the exposure (Schönborn et al. 2000).)

In the validation measurements, the input power to the TEM cell was set at 113.5 W. Fluoroptic immersion temperature probes (Luxtron unit 790, probe type SFF) were chosen, as there are no metallic components to produce interference with the  $E$ -field. Measurements were performed when the two flasks, each filled with 6 mm high medium were placed in the TEM cell, and then again when the two flasks each had 12 mm of medium. The medium consisted of RPMI in a gelled form (using Natrosol 250 HR, 7.4% by mass) to reduce the effect of thermal diffusion due to convection (no cell culture was present). The measured electrical conductivity of the gel (with added common salt, 0.21% by mass, to obtain comparable conductivity to liquid RPMI) was 2.05 S/m and the relative permittivity 72.6. The measurements were performed in an environment that was not temperature controlled. These conditions were not sufficient to accurately determine local SAR from  $\partial T/\partial t$  alone, since the chosen temperature probes have inadequate sensitivity at this power level.

Thermal modelling was undertaken through the development of a finite-difference temperature modelling environment based on equation 3 (using the numerical formulation in Wang and Fujiwara 1999, with the XFDTD mesh), and where, in addition, the thermal conditions at the surface are modelled as a convective boundary:

$$K \frac{\partial T}{\partial n} = -h(T - T_a) \quad (4)$$

where  $h$  is the convection coefficient, and  $T_a$  is the ambient temperature. For the RPMI gel, the specific heat capacity,  $c$ , was set at 4174 J/(kg °C), and the thermal conductivity,  $K$ , was set at 0.60 W/(m °C) (as for water). The convection coefficient,  $h$ , was set at 10.5 W/(m<sup>2</sup> °C) (see Kritikos et al. 1981, and Wang and Fujiwara 1999). The increase in ambient temperature in the TEM cell,  $T_a$ , was accounted for (for empty flasks, measurements showed a 0.16 °C increase over 360 s).

The input SAR profile is first calculated in XFDTD. As well as the mesh described previously for the 6 mm high medium, a second mesh was created for a 12 mm high medium (with cubical cells of length 1.0 mm). The measured values for the conductivity and relative permittivity of the RPMI gel were used. The calculations found that, with an input of 113.5 W, the peak SAR on the bottom of the 6 mm and 12 mm medium is 9.25 W/kg and 67.59 W/kg, respectively. The SAR profile was then input to the thermal model.

Figure 6 presents a comparison of two temperature measurements with the temperatures calculated by the model. The agreement between the results provides confidence in the accuracy of the SAR values. Other measurements gave consistent results. Due to thermal

conduction processes, the temperature rise profile at any given height in the medium has a similar shape over the 360 s period to that shown in Figure 6 (apart from the deviation in the first few seconds due to the particular SAR at that position, which cannot be resolved in our measurements) (see also Pickard et al. 1999 and Samaras et al. 2000). However, this type of long term comparison does confirm the average SAR value, and by using this as a reference, also confirms the value of SAR

throughout the height (given our confidence in the shape of the vertical profile as discussed above).

The temperature program was also used to confirm that for 2.5 W input, the exposure is under what is deemed ‘athermal’ conditions (the peak steady-state temperature rise is estimated to be only 0.013°C).

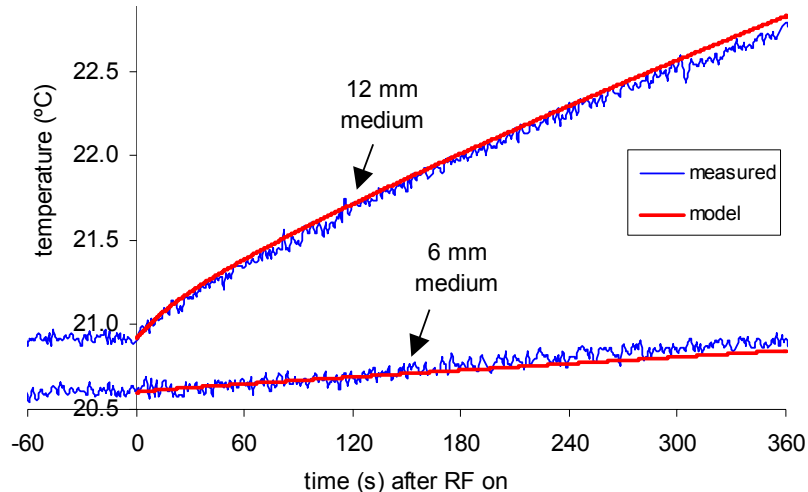


Figure 6. Comparison of measured and model temperature rise (0.5 mm off the bottom in the centre) for 113.5 W input

## 6. Conclusions

*In vitro* studies present a significant challenge to researchers in ensuring that the SAR of the exposed cell culture is accurately characterised. A TEM cell exposure chamber provides a useful system for *in vitro* studies due to the uniform layer in the medium where the cell culture resides. However, due to the highly non-uniform SAR profile in the vertical direction in the medium, it is critical that accurate techniques are employed to obtain an accurate estimate of the SAR. This paper has shown how this can be provided through the development of SAR and temperature computational analysis methods, both in the estimation and validation process.

## References

- Burkhardt M, Pokovic K, Gnos M, Schmid T, and Kuster N, “Numerical and Experimental Dosimetry of Petri Dish Exposure Setups”, *Bioelectromagnetics*, Vol 17, pp483-493, 1996.
- Crawford M L, “Generation of Standard EM Fields using TEM Transmission Cells”, *IEEE Transact EMC*, Vol 16, No 4, pp189-195, 1974.
- Crawford M L, and Workman J L, “Using a TEM Cell for EMC Measurements of Electronic Equipment”, *US Department of Commerce, National Bureau of Standards, Technical Note 1013*, Apr 1979.
- French P W, and Blood A, “Characterisation of Molecular Changes Induced by Simulated Mobile Phone Radiofrequency Radiation Exposure”, *2<sup>nd</sup> Intl Workshop on Biological Effects of EMFs*, Greece, 2002.
- Gabriel C, “Compilation of the Dielectric Properties of Body Tissues at RF and Microwave Frequencies”, *Brooks Air Force Technical Report AL/OE-TR-1996-0037* (see <http://www.fcc.gov/fcc-bin/dielec.sh>, accessed July 2003).
- Guy A W, Chou C K, and McDougall J A, “A Quarter Century of *in vitro* Research: A New Look at Exposure Methods”, *Bioelectromagnetics*, Vol 20, pp21-39, 1999.
- Kritikos H N, Foster K R, and Schwan H P, “Temperature Profiles in Spheres Due to Electromagnetic Heating”, *J Microwave Power*, Vol 16, No 3-4, pp327-344, 1981.
- Kunz K S, and Luebbers R J, “The Finite Difference Time Domain Method for Electromagnetics”, *CRC Press*, 1993.

Kuster N, and Schönborn F, "Recommended Minimal Requirements and Development Guidelines for Exposure Setups of Bio-Experiments Addressing the Health Risk Concern of Wireless Communication", *Bioelectromagnetics*, Vol 21, pp508-514, 2000

Moros E G, and Pickard W F, "On the Assumption of Negligible Heat Diffusion during the Thermal Measurement of a Nonuniform Specific Absorption Rate", *Rad Res*, Vol 152, pp312-320, 1999

Pickard W F, Straube W L, Moros E G, and Fan X, "Simplified Model and Measurement of a Specific Absorption Rate Distribution in a Culture Flask Within a Transverse Electromagnetic Mode Exposure System", *Bioelectromagnetics*, Vol 20, pp183-193, 1999.

Popovic M, Hagness S C, and Taflove A, "Finite-Difference Time-Domain Analysis of a Complete Transverse Electromagnetic Cell Loaded with Liquid Biological Media in Culture Dishes", *IEEE Trans Biomedical Eng*, Vol 45, No 8, Aug 1998.

Remcom, Inc. website <http://www.remcom.com>. Accessed July 2003.

Rowley J T, and Anderson V, "A Critical Review of Resonant Cavities for Experimental *in vitro* Exposure to Radiofrequency Fields", *Inaugural Conf of IEEE EMBS Australia*, pp150-153, Feb 1999.

Samaras T, Regli P, and Kuster N, "Electromagnetic and Heat Transfer Computations for Non-ionizing Radiation Dosimetry", *Phys Med Biol*, Vol 45, pp2233-2246, 2000.

Schönborn F, Pokovic K, Burkhardt M, and Kuster N, "Basis for Optimization of *in vitro* Exposure Apparatus for Health Hazard Evaluations of Mobile Phone Communications", *Bioelectromagnetics*, Vol 22, pp547-559, 2001.

Schönborn F, Pokovic K, Wobus A M, and Kuster N, "Design, Optimisation, Realization, and Analysis of an In Vitro System for the Exposure of Embryonic Stem Cells at 1.71 GHz", *Bioelectromagnetics*, Vol 21, pp372-384, 2000.

Schuderer J, and Kuster N, "Effect of the Meniscus at the Solid/Liquid Interface on the SAR Distribution in Petri Dishes and Flasks", *Bioelectromagnetics*, Vol 24, pp103-108, 2003.

Wang J, and Fujiwara O, "FDTD Computation of Temperature Rise in the Human Head for Portable Phones", *IEEE Trans Microwave Theory and Techniques*, Vol 47, No 8, Aug 1999, pp1528-1534.



Robert McIntosh obtained his PhD in Mathematics at the Australian National University in 1989 in the area of PDEs. He has been a member of the Electromagnetic Energy (EME) Safety Research team at Telstra Research since 1999, developing and applying a numerical modelling environment for the study of RF dosimetry and human body absorption. Between 1989 and 1999, he worked at the BHP Research Laboratories on the development of electromagnetic levitation, pumping, and braking devices for liquid metal, and new techniques in noise reduction in electromagnetic geophysics. Robert is a member of the Australian Mathematical Society.



Ray McKenzie is the Project Leader of the EME Safety Research Group at the Telstra Research Laboratories (TRL), where he leads a team of researchers investigating the effects of human exposure to electromagnetic energy (EME). He specialises in electromagnetic propagation and physical interactions, in particular the dosimetry and measurement of ambient fields and SAR, as well as computational electromagnetic modelling. He has spent 13 years in the area of electromagnetic energy and is in his 20<sup>th</sup> year at TRL. He gained his Bachelor of Applied Science with first class honours in Physics from RMIT University in 1996, and currently undertakes postgraduate research in radon dosimetry at the Whole Body Facility of the Australian Radiation Protection and Nuclear Safety Agency (ARPANSA). He currently serves on specialist working committees of the Australian Communications Authority (ACA), the Australian Communications Industry Forum (ACIF), the Australian Mobile Telephone Association (AMTA) and the IEEE International Committee on Electromagnetic Safety (ICES) Standards Committee 4. Ray is a member of the Applied Computational Electromagnetic Society (ACES) and the Bioelectromagnetics Society (BEMS).



Steve Iskra received the B.E. (Hon.) degree in electrical engineering from the University of Melbourne, Australia in 1982. In 1982 he joined the Telstra Research Laboratories and has specialised in the areas of EMC and in the interaction of radio waves on the human body and on medical devices. He is a member of the International Special Committee on Radio Interference (CISPR) and Committee TE/3,

Electromagnetic Interference, of Standards Australia.



Amico Carratelli is a senior technical officer in the EME Safety Group at the Telstra Research Laboratories. Amico received an Associate Diploma in Mechanical Engineering in 1991 and has also completed Certificate of Technology courses in Mechanical Design (1974) and Structural Design (1980).

Amico has extensive research and development experience in the design/manufacture and analytical assessments of mechanical and electromechanical systems. He has lead project teams in evaluation of new telecommunications technologies and technology deployment across the company. Amico is currently assisting research teams with the main focus being SAR measurement techniques and SAR hardware development and implementation.



Paul Standaert received an Honours Degree in Electrical Engineering from Deakin University in 1982. He started work with the then Telecom Australia Research Laboratories as a Research Engineer in 1982.

Paul has worked in designing automated measurement instrumentation, has run the laboratories asset acquisition programme, and has also assisted in the development of optical standards for Telstra. His current research interests are in speech quality in communication systems as well as EME general research and measurement systems.